Applied Surface Science 258 (2012) 10123–10127

Applied Surface Science

journal homepage: www.elsevier.com/locate/apsusc

Monitoring preparation and phase transitions of carburized W(1 1 0) by reflectance difference spectroscopy

Magdalena Bachmann[a], Norbert Memmel[a,*], Erminald Bertel[a], Mariella Denk[b], Michael Hohage[b], Peter Zeppenfeld[b]

[a] Institute of Physical Chemistry, University of Innsbruck, Innrain 52a, A-6020 Innsbruck, Austria
[b] Institute of Experimental Physics, Johannes Kepler University Linz, Altenbergerstr. 69, A-4040 Linz, Austria

ARTICLE INFO

Article history:
Received 12 April 2012
Received in revised form 1 June 2012
Accepted 24 June 2012
Available online 2 July 2012

Keywords:
Reflectance difference spectroscopy
Tungsten
Carbon
Phase transition
Auger-electron spectroscopy
Low-energy electron diffraction

ABSTRACT

Reflectance difference spectroscopy (RDS) is applied to follow in situ the preparation of clean and carburized W(1 1 0) surfaces and to study the temperature-induced transition between the R(15 × 3) and R(15 × 12) carbon/tungsten surface phases. RDS data for this transition are compared to data obtained from Auger-electron spectroscopy and low-energy electron diffraction. All techniques reveal that this transition, occurring around 1870 K, is reversible with a small hysteresis, indicating a first-order-like behaviour. The present results also prove a high surface sensitivity of RDS, which is attributed to the excitation of electronic p-like surface resonances of W(1 1 0).

1. Introduction

As surface science matures, it more and more evolves from the study of solid/vacuum interfaces towards investigation of practically more relevant solid/liquid- or solid/gas-interfaces with gas pressures close to ambient pressure. As most surface science techniques involve particles as probes which strongly interact with matter, their applicability to such "real" systems is strongly hampered. Alternatively non-linear optical methods can be applied, because they are surface sensitive but do not suffer from this drawback. However, in case of anisotropic surfaces on isotropic bulk substrates, linear optical methods can be used as well. Clearly, if for such a system an optical anisotropy is detected, it has to originate from the surface. This idea is the basis of reflectance difference spectroscopy (RDS) or reflectance anisotropy spectroscopy (RAS), as it is also called. Here linearly polarized light, with the polarization direction oriented at 45° relative to the two principal non-equivalent orthogonal directions x and y of the anisotropic surface, impinges at normal incidence and the difference of the complex reflectances r_x and r_y of both polarization components is measured by applying phase-modulation techniques [1–3]. The complex normalized reflectance difference is defined as:

$$\frac{\Delta r}{r} = 2\frac{r_x - r_y}{r_x + r_y}, \quad (1)$$

both the real and imaginary part of which can be measured as a function of the frequency of the incoming light. Whereas the real part of Δr describes the different reflection amplitudes of x- and y-polarized light, the imaginary part is related to the different phase shifts experienced by the two polarization components upon reflection. However, as discussed in Ref. [2] the microscopic interpretation and theoretical calculation of the surface optical response from first principles is still a challenging task. For a detailed discussion of the RDS technique, its physical background and theoretical description we refer to the existing literature [1–3].

Although originally developed for investigation of semiconductor surfaces, the technique can be and has been applied to metal surfaces as well. It has been shown, that the technique is very surface-sensitive, in particular, if the optical excitations involve electronic surface states or resonance states which are localized in the surface-near region.

Since RDS is an optical and thus contactless technique, it is especially suited to investigate processes at high temperatures. However, in such a case one should be aware that the RDS intensity may show temperature-dependent changes due to

* Corresponding author.
E-mail address: norbert.memmel@uibk.ac.at (N. Memmel).

0169-4332
http://dx.doi.org/10.1016/j.apsusc.2012.06.089

several mechanisms, which might not directly reflect the process the user is interested in. These mechanisms include thermal expansion and associated changes in surface electronic structure, enhanced vibrations, disorder or change of morphology [1,2], as well as broadening of the Fermi-function (if electronic states close to the Fermi-level are involved) or – at sufficiently high temperatures – radiation emitted by the sample in the frequency range detected in RDS. These problems can be circumvented by performing kinetic measurements at fixed temperatures.

In the present paper RDS is used to follow the preparation of clean and carburized W(1 1 0) surfaces and the temperature-induced first-order transition between the high-coverage R(15 × 3)-C/W(1 1 0) and the low-coverage R(15 × 12)-C/W(1 1 0) phase. By comparison with Auger-electron spectroscopy (AES) and low-energy electron diffraction (LEED) data the excellent surface-sensitivity of RDS is demonstrated.

Although both carbon superstructures were reported already in the 1960s [4,5], their precise atomic structure is still unclear. This is mostly due to the large size of the unit cells, involving 15 or 60 tungsten surface atoms per R(15 × 3) or R(15 × 12) unit cell, respectively (note that the notation is for historical reasons and does not follow the standard Wood convention). With scanning tunnelling microscopy (STM) atomic-scale details were resolved on the R(15 × 3) surface and interpreted as 6 carbon atoms per unit cell, organized in short rows arranged in a zigzag manner [6,7]. For the (15 × 12) surface in some parts of the large unit cell STM revealed an atomic pattern similar to that of clean W(1 1 0), indicating that small patches of nearly unperturbed W(1 1 0) exist within each (15 × 12) unit cell [6]. The AES segregation analysis of Foulias et al. indicates that the carbon coverage in the R(15 × 12) structure is about one third of that of the R(15 × 3) phase [8]. Due to the mirror symmetry of the tungsten substrate two symmetry-equivalent domains exist for each structure. Recently, it was demonstrated, that these long-range-ordered carburized surfaces form excellent highly temperature-stable templates for metal cluster deposition, which may have interesting practical applications [9–11].

2. Experiment

Experiments were carried out in an UHV-system with a base pressure of 1×10^{-10} mbar. The RD spectrometer of the Aspnes type [12] was attached to the chamber through a strain-free optical window. The normalized reflectance difference (with $r_x = r_{[0\,0\,1]}$ and $r_y = r_{[\bar{1}\,1\,0]}$) was recorded for photon energies between 1.5 and 5 eV. Auger-electron spectra were acquired using a normal-incidence 2 keV electron beam and a 4-grid LEED/AES retarding field analyzer for detection of the carbon 272 eV and tungsten 169 eV Auger electrons. Electron diffraction patterns were recorded at low electron energies (20 eV) to allow for a better resolution of the closely-spaced carbon-induced superstructure spots. The sample was a circular disk of 8 mm diameter and could be heated by electron-bombardment up to 2700 K. Sample temperatures above 1000 K were monitored with a two-colour pyrometer. The preparation of clean and carburized W(1 1 0) will be described in the following section in connection with the RDS measurements. Gas pressures given in this paper are direct "nitrogen-equivalent" readings from the Bayard-Alpert ionization gauge, whereas for calculation of gas exposures the pressure readings were multiplied with the gas correction factors for O_2 ($f_{O_2} = 0.99$) and C_2H_4 ($f_{C_2H_4} = 0.43$). Gas exposures are specified in Langmuir ($1\,L = 10^{-6}$ torr s). Coverages are given in monolayers with one monolayer (ML) corresponding to the density of W(1 1 0) surface atoms (1.42×10^{19} atoms/m^2).

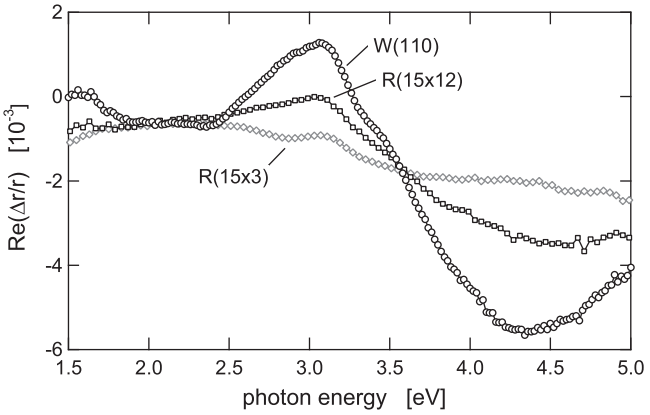

Fig. 1. RDS spectra of clean W(1 1 0) and carburized W(1 1 0) in the low-coverage R(15 × 12) and high coverage R(15 × 3) phase. The clean surface was measured at 100 K, the carburized surfaces at 300 K.

3. Results and discussion

3.1. RD spectra of clean and carburized W(1 1 0)

Fig. 1a shows a comparison of the real part of RD spectra of clean W(1 1 0) and of the surface covered with the low-coverage R(15 × 12) and the high-coverage R(15 × 3) carbon phases. The spectrum of the clean surface exhibits a pronounced maximum at a photon energy of 3.05 eV and a minimum around 4.35 eV. Both structures are well known from previous experimental and theoretical RDS work on W(1 1 0). As shown by theory, the maximum in Re ($\Delta r/r$) is associated with transitions from p-like to d-like electronic states [13]. The p-like states have a strong surface resonance character, making the associated RD feature particularly sensitive to surface modifications. This is in agreement with experimental data, showing that adsorption of oxygen or deposition of thin silver or iron overlayers result in a quenching of the RDS intensity at 3.05 eV [14–16]. As is evident from Fig. 1, the same quenching behaviour is also observed upon carburization of the W(1 1 0) surface. With increasing carbon surface content the maximum at 3.05 eV drops in intensity. The minimum at 4.35 eV is suppressed about equally strong, paralleling experiments were overlayers of iron or silver were deposited [14,15]. These observations indicate that the 4.35 eV feature exhibits a surface sensitivity comparable to that of the 3.05 eV feature, although this conclusion is at variance with the theoretical explanation given by Ammi et al. [13]. As can be seen from Fig. 1 carbon deposition onto the surface essentially results in a quenching of the clean surface features over the entire measured photon energy range without introducing new characteristic RDS features.

Motivated by the well-established surface sensitivity of the 3.05 eV feature we will in the following use the intensity at this photon energy for in situ monitoring of surface modifications during preparation of clean and carburized W(1 1 0).

3.2. Monitoring surface preparation

Tungsten has the highest melting point of all elemental solids and a low vapour pressure. Thus it can be cleaned from most impurities simply by annealing to very high temperatures (above ≈ 2000 K) where these impurities desorb. However, this procedure does not work for carbon, which can withstand the high-temperature treatment. Hence carbon impurities have to be removed by "medium"-temperature oxidation [17]. In Fig. 2 this oxidation is followed by RDS, starting from a carbon-contaminated W(1 1 0) surface. Upon exposure to oxygen

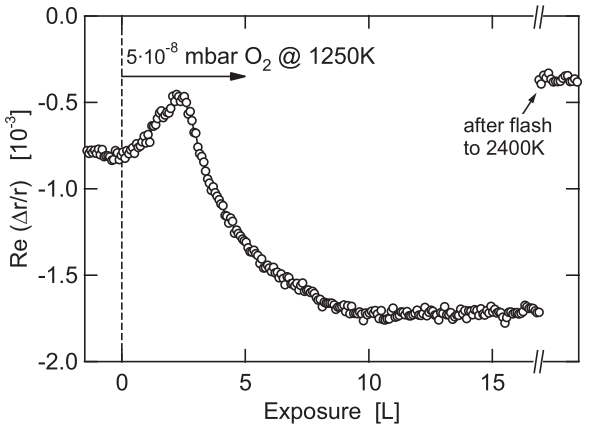

Fig. 2. RDS-intensity at 3.05 eV during exposure of a carbon-contaminated W(1 1 0) surface to oxygen (T = 1250 K).

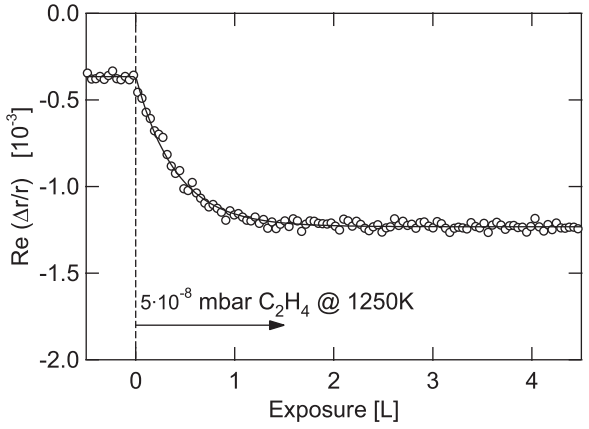

Fig. 3. RDS-intensity at 3.05 eV during preparation of a carbon-saturated R(15 × 3) surface by exposure to C_2H_4 at 1250 K. The solid line is a fit to an exponential decay, yielding a decay constant $k = 2.44\,L^{-1}$.

atmosphere ($p = 5 \times 10^{-8}$ mbar, sample temperature 1250 K) the RD intensity at 3.05 eV starts to rise, indicating removal of carbon from the surface due to formation and desorption of CO. The RD signal then reaches a maximum with a signal strength close to that of clean W(1 1 0), before it starts to decline towards a constant low level at long oxygen exposures. We suppose that at the point of maximum intensity essentially all carbon is removed from the surface. Beyond this point the W(1 1 0) surface gets oxidized, leading to the observed reduction in RD intensity which proceeds until the surface is fully covered with oxygen. The surface oxide thus formed can be removed by heating the sample to high temperatures (≈2400 K) [17]. Indeed, upon flashing the sample to 2400 K the RD intensity at 3.05 eV is recovered and the RD spectrum characteristic of the clean, well-ordered surface is obtained (see Fig. 1). The final RD intensity in Fig. 2 is slightly higher than the value measured at the point of the maximum. This difference is attributed to an improved surface ordering after the high-temperature flash. The thus prepared sample exhibited an extremely sharp (1 × 1) LEED pattern and only a minor AES carbon signal. We attribute this residual signal to carbon atoms in deeper layers, which are difficult to remove completely, especially if – as in the present series of carburization experiments – the sample is (on purpose) regularly exposed to external sources of carbon. STM measurements of the cleaned surface did not show signs of carbon-induced R(15 × 12) islands, which usually exist at low carbon coverages. Hence we conclude that the surface itself is essentially free of carbon after the cleaning procedure.

In order to carburize the W(1 1 0) surface in a controlled manner, the clean surface was exposed to a carbon-containing feed gas at sample temperatures sufficiently high to allow for a cracking of the feed gas molecules. In the present case ethene (C_2H_4) was used as the feed gas at a pressure of 5×10^{-8} mbar and a sample temperature of 1250 K. It should however be noted that other hydrocarbon gases work as well [7,11,18]. As can be seen from Fig. 3 and as expected from the spectra shown in Fig. 1, carbon deposition results in a decreasing RDS signal. After an exposure of ≈ 1.5 L a virtually constant value is reached as the surface becomes saturated with carbon. The observed exponential decrease is in full agreement with previous AES adsorption studies of Macmillan et al., implying that the RD signal is linearly connected to the carbon-content as determined in Ref. [18]. The first-order decay suggests that the adsorption rate is limited by the impingement of C_2H_4 molecules on W(1 1 0), rather than by the dissociation process itself. In this case the rate constant k is given by (Langmuir model):

$$k = \frac{2}{\sqrt{2\pi m k_B T}} \times \frac{s_0}{N_{sat}} \quad (2)$$

where m is the mass of the ethene molecules, k_B the Boltzmann constant, T the gas temperature (300 K), s_0 the initial sticking coefficient and N_{sat} the number of carbon atoms per unit area at saturation [18]. The factor of two accounts for the occupation of two adsorption sites due to dissociative adsorption. Taking $k = 2.44\,L^{-1}$ from the exponential fit to the data in Fig. 3 and assuming unity sticking coefficient, the saturation coverage N_{sat} can be calculated from Eq. (2). A value of 0.22 ML is obtained, clearly lower than the values of 0.6–0.7 ML given in Refs. [8,18], but in reasonable agreement with the above-mentioned STM-deduced model of 6 carbon atoms per 15 tungsten surface atoms, i.e. 0.4 ML [7].

For completeness we would like to note that the absolute numbers of the RDS intensity given in Fig. 3 differ from the values recorded in Fig. 1 as a consequence of the different measurement temperatures (1250 K in Fig. 3 vs. 100 K and 300 K in Fig. 1).

Figs. 2 and 3 demonstrate convincingly that RDS is well suited for monitoring surface modifications even under restrictive conditions of elevated sample temperatures and gas pressures. In the present case, data were obtained at a gas pressure where other surface sensitive techniques like electron spectroscopies could have been used as well. Note however, that higher pressures – incompatible with standard electron spectroscopy setups – would not hamper the RDS measurement. As RDS is sufficiently quick for real-time diagnostics it allows to easily optimize the preparation process. Obviously in the procedure used in Fig. 2 the sample was severely overdosed with oxygen. A better and more effective procedure would be to stop oxygen exposure at the point of maximum RDS intensity (i.e. at ≈ 2.4 L), followed by a short high-temperature flash to improve the surface order. Analogously from Fig. 3 it can be concluded that an exposure of ≈ 1.5 L would have been sufficient for saturation of W(1 1 0) with carbon.

3.3. The R(15 × 13)-R(15 × 12) transition

The transition from the high-coverage R(15 × 3) phase to the low-coverage R(15 × 12)-C/W(1 1 0) phase was investigated by annealing a carbon-saturated W(1 1 0) surface (prepared by exposure to ≈ 9 L of ethene at 1250 K) for 10 min at various temperatures. For $T \geq 2200$ K only 3 min annealing time was used to reduce the thermal load to the manipulator. After each annealing step the sample was rapidly quenched to 1250 K, in order to freeze the high-temperature situation. The RD intensity was then recorded at 1250 K, using a photon energy of 3.05 eV. In principle the RD intensity can be (and actually has also been) followed during the annealing process. However, since – as discussed in the introduction – the RD signal itself changes with temperature due to several

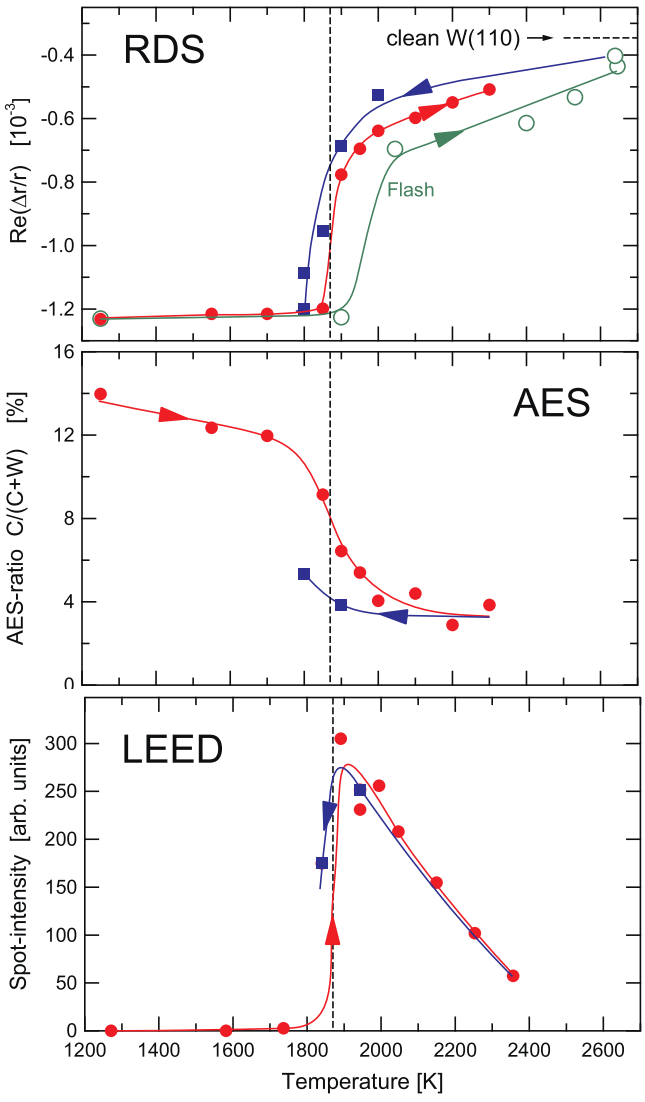

Fig. 4. RDS, carbon-AES and R(15 × 12) LEED intensity upon annealing and cooling of a carbon-saturated W(1 1 0) surface. Filled red circles are measured after successive step-wise annealing (10 min at each temperature, only 3 min for T ≥ 2200 K), blue squares are data after recooling samples that have been subjected to a higher temperature before. Open green circles are from samples that have been flashed (for ≈ 1–2 s) to the indicated temperature. Solid lines are guides to the eye.

mechanisms, the intensity was evaluated at the fixed reference temperature of 1250 K. The corresponding data points are shown as the filled red circles in the upper panel of Fig. 4. The RD intensity stays virtually constant up to an annealing temperature of 1850 K. Between 1850 and 1900 K a rapid rise is observed, indicating the transition from the high-coverage R(15 × 3) to the low-coverage R(15 × 12) phase with rapid dissolution of the excess surface carbon into the bulk of the tungsten substrate [5,8,18,19]. For temperatures beyond 1900 K the RDS signal increases slowly but steadily towards the clean surface value, suggesting a continuously decreasing average carbon surface concentration in this temperature region.

Upon recooling the opposite behaviour is observed with a small hysteresis of ≈ 50 K. The inverted behaviour clearly demonstrates that the transition between both carbon structures is a reversible process, in agreement with the early reports of Baudoing and Stern [5] and Foulias et al. [8]. The reversibility also implies that (i) observation of the high-temperature, low-coverage R(15 × 12) structure at low temperatures is only possible by rapid quenching and that (ii) the precise value of the measured transition temperature (≈ 1870 K in Fig. 4) depends on the cooling rate used to quench the sample from high temperatures to the measurement temperature of 1250 K. The observation of a hysteresis (which so far has not been reported in the literature) is particularly noteworthy, as the RD intensity recorded during each annealing step had always reached a practically stationary level. Hence the hysteresis would also persist, if much longer annealing times were used. Accordingly, the observed hysteresis is a genuine feature of the R(15 × 3)–R(15 × 12) transition, indicating that the transition is of first order, since hysteresis curves are characteristic hallmarks of first-order phase transitions. Obviously, the conversion from the R(15 × 3) to the R(15 × 12) structure (and vice versa) does not take place by a continuous decrease or increase of the local carbon coverage. Rather, evolution of the new phase requires the occurrence of nucleation events, which are responsible for the observed hysteresis.

If the carbon-saturated surface is heated by short flashes (≈ 1–2 s) to the desired temperature rather than by annealing for 10 min, dissolution of surface carbon into the bulk is not fast enough to reach the thermodynamically favoured state. Accordingly, the observed transition point is shifted to considerably higher temperatures (open green circles in Fig. 4).

It is instructive to compare the RDS results with the surface and surface-near carbon content as obtained by Auger-electron spectroscopy (AES), see centre panel of Fig. 4. The AES-ratios $I_C/(I_C + I_W)$ were obtained using analogous annealing/cooling procedures as for the RDS measurements; the only difference was that the Auger spectra were recorded at 500 K, rather than at 1250 K as in case of RDS. Similar to the RDS measurements AES indicates a rapid change from the high-coverage R(15 × 3) phase to the low-coverage R(15 × 12) structure at a temperature of 1870 K. The hysteresis behaviour is observed as well. However, the transition between both structures is more washed out in the AES data. In particular, in the temperature region below the transition point, where the RDS signal is almost perfectly constant, AES measures a slowly but clearly decreasing carbon content, indicating that carbon loss to the tungsten bulk does already take place in this temperature region. We associate these dissolving atoms with carbon atoms which already moved into subsurface (near-surface) layers during preparation of the carburized surface at exposures exceeding 1.5 L, where the surface is already saturated with carbon, see Fig. 3). Obviously, these subsurface atoms are not detected by RDS, indicating that in the present experiment RDS is essentially sensitive to surface carbon only, whereas the information depth of AES comprises several layers (the inelastic mean free paths for the W(169 eV) and C(272 eV) Auger electrons are ≈ 0.5–0.6 nm [20]). The "invisibility" of subsurface carbon to RDS is plausible due to the more isotropic environment in subsurface layers as compared to the topmost layer. At first sight the different behaviour of RDS and AES signals seems to contradict our finding in Section 3.2 that the RD intensity scales linearly with the AES signal measured by Macmillan during adsorption [18]. However, the adsorption run of Macmillan was made at lower temperature (1100 K), where supposedly carbon-diffusion into subsurface layers is kinetically hindered. The build-up of subsurface carbon at our deposition temperature of 1250 K was verified by increasing the C_2H_4 pressure and exposure: in case of extremely high pressures/exposures only the R(15 × 3) structure could be observed by LEED, even after heating to quite high temperatures, indicating that the equilibrium R(15 × 3) ⇌ R(15 × 12) + C_{bulk} was severely shifted towards the R(15 × 3) side by a high concentration of subsurface/bulk-dissolved carbon atoms C_{bulk}. This finding is in agreement with earlier studies stating that for W(1 1 0) crystals with a high (bulk) carbon content the R(15 × 12) structure cannot be observed at all [8].

Finally the transition between both surface phases was also followed by low-energy electron diffraction (LEED). The heating/cooling procedure of the sample was again similar as for the RDS

and AES measurements. For recording the LEED images the sample was quenched to below room-temperature. The lower panel of Fig. 4 shows the intensity of the (17/60, 2/5) LEED spot, which is characteristic of the R(15 × 12) phase [21]. The observed behaviour is quite analogous to that of the RD signal: a constant value at "low" temperatures, followed by a rapid rise at the transition temperature and a continuous decay as the surface approaches the clean state at high temperatures. However, it should be mentioned that – although no distinct R(15 × 12) diffraction spots are visible below the transition temperature – the LEED pattern nevertheless shows some changes. Around 1700 K the diffraction pattern becomes streaky. Out of these streaks the R(15 × 12)-spots evolve at $T > 1870$ K. The hysteresis behaviour cannot be discerned so clearly from the LEED data, due to the low number of data points and their relatively strong scatter.

4. Summary

In conclusion, the present work demonstrates the applicability of RDS for in situ monitoring of surface processes such as adsorption, desorption or phase transitions. Selected spectral features can serve as finger prints which allow to follow the kinetics of these processes in situ and in real-time. As RDS is an optical technique it can even be applied to study processes under rather harsh environmental conditions, such as high gas pressures or high temperatures. As example in the present work the high-temperature phase transformation occurring around 1870 K between the R(15 × 3) and the R(15 × 12) carbon surface phases was followed and shown to be reversible in nature. A small hysteresis was observed, providing evidence that the phase transition is of first-order type. Furthermore, comparison of RDS with data acquired by AES and electron diffraction shows that, if electronic surface states or surface resonances are involved in the optical excitation, RDS can attain a very high surface sensitivity that may exceed that of Auger-electron spectroscopy.

Acknowledgements

Financial support by the Austrian Science Fund (grant S9004-N20) and the Austrian Academy of Sciences is gratefully acknowledged. We thank Reinhold Pramsoler for his excellent technical assistance.

References

[1] D.S. Martin, P. Weightman, Surface and Interface Analysis 31 (2001) 915.
[2] P. Weightman, D.S. Martin, R.J. Cole, T. Farrell, Reports on Progress in Physics 68 (2005) 1251.
[3] M. Hohage, L.D. Sun, P. Zeppenfeld, Applied Physics A 80 (2005) 1005.
[4] E. Bauer, Surface Science 7 (1967) 351.
[5] R. Baudoing, R.M. Stern, Surface Science 10 (1968) 392.
[6] M. Bode, R. Pascal, R. Wiesendanger, Surface Science 344 (1995) 185.
[7] A. Varykhalov, O. Rader, W. Gudat, Physical Review B 72 (2005) 115440.
[8] S.D. Foulias, K.J. Rawlings, B.J. Hopkins, Journal of Physics C: Solid State Physics 14 (1981) 5403.
[9] V. Varykhalov, O. Rader, W. Gudat, Physical Review B 77 (2008) 035412.
[10] M. Bachmann, M. Gabl, C. Deisl, N. Memmel, E. Bertel, Physical Review B 78 (2008) 235410.
[11] M. Bachmann, N. Memmel, E. Bertel, Surface Science 605 (2011) 1263.
[12] D.E. Aspnes, J.P. Harbison, A.A. Studna, L.T. Florez, Journal of Vacuum Science & Technology A 6 (1988) 1327.
[13] D. Ammi, A. Ziane, S. Bouarab, Surface Science 554 (2004) 60.
[14] D.S. Martin, O. Zeybek, B. Sheridan, S.D. Barrett, P. Weightman, J.E. Ingelsfield, S. Crampin, Journal of Physics: Condensed Matter 13 (2001) L607.
[15] L.D. Sun, M. Hohage, P. Zeppenfeld, C. Deisl, E. Bertel, Surface Science 600 (2006) L281.
[16] D.S. Martin, O. Zeybek, P. Weightman, S.D. Barrett, Journal of Physics: Condensed Matter 23 (2011) 355002.
[17] R.G. Musket, W. McLean, C.A. Colmenares, D.M. Makowiecki, W.J. Siekhaus, Applications of Surface Science 10 (1982) 143.
[18] J.G. Macmillan, A.J. Slavin, K.J. Sunderland, Surface Science 173 (1986) 138.
[19] K.J. Sunderland, A.J. Slavin, Surface Science 233 (1990) 89.
[20] C.J. Powell, A. Jablonski, NIST Electron Effective Attenuation-Length Database, Version 1.1, National Institute of Standards and Technology, Gaithersburg, MD, 2003.
[21] LEED-spot notation is based on the reciprocal lattice vectors **b**1 and **b**2 as specified in M. Gabl, M. Trzcinski, N. Memmel, A. Bukaluk, E. Bertel, Surface Science 600 (2006) 4390.